Human Molecular Genetics, 2015, Vol. 24, No. 25 7171–7181

doi: 10.1093/hmg/ddv414
Advance Access Publication Date: 6 October 2015
Original Article

ORIGINAL ARTICLE

Increased *STAG2* dosage defines a novel cohesinopathy with intellectual disability and behavioral problems

Raman Kumar[1], Mark A. Corbett[1], Bregje W.M. Van Bon[2], Alison Gardner[1], Joshua A. Woenig[1], Lachlan A. Jolly[1], Evelyn Douglas[3], Kathryn Friend[3], Chuan Tan[1], Hilde Van Esch[4], Maureen Holvoet[4], Martine Raynaud[5], Michael Field[6], Melanie Leffler[6], Bartłomiej Budny[7], Marzena Wisniewska[8], Magdalena Badura-Stronka[8], Anna Latos-Bieleńska[8], Jacqueline Batanian[9], Jill A. Rosenfeld[10,14], Lina Basel-Vanagaite[11], Corinna Jensen[12], Melanie Bienek[12], Guy Froyen[16], Reinhard Ullmann[12,17], Hao Hu[12], Michael I. Love[13], Stefan A. Haas[13], Pawel Stankiewicz[14], Sau Wai Cheung[14], Anne Baxendale[15], Jillian Nicholl[3], Elizabeth M. Thompson[1,15], Eric Haan[1,15], Vera M. Kalscheuer[12] and Jozef Gecz[1,*]

[1]School of Medicine, and the Robinson Research Institute, The University of Adelaide, Adelaide, SA 5000, Australia, [2]Radboud University Medical Center, 6525 GA, Nijmegen, The Netherlands, [3]Genetics and Molecular Pathology, SA Pathology, North Adelaide, SA 5006, Australia, [4]Center for Human Genetics, University Hospitals Leuven, 3000 Leuven, Belgium, [5]Centre Hospitalier Régional Universitaire, Service de Génétique, 37000 Tours, France, [6]Genetics of Learning Disability Service, Hunter Genetics, Waratah, NSW 2298, Australia, [7]Department of Endocrinology, Metabolism and Internal Diseases and, [8]Department of Medical Genetics, Poznan University of Medical Sciences, Poznan 60-355, Poland, [9]Department of Pediatrics, Saint Louis University, St Louis, MO 63104, USA, [10]Signature Genomic Laboratories, Spokane, WA 99207, USA, [11]Raphael Recanati Genetic Institute and Felsenstein Medical Research Center, Rabin Medical Center, Beilinson Campus, Petah Tikva 49100, Israel, [12]Department of Human Molecular Genetics and, [13]Department of Computational Molecular Biology, Max Planck Institute for Molecular Genetics, Ihnestrasse 73, 14195 Berlin, Germany, [14]Department of Molecular and Human Genetics, Baylor College of Medicine, Houston, TX 77030, USA, [15]South Australian Clinical Genetics Service, SA Pathology, North Adelaide, SA 5006, Australia, [16]Human Genome Laboratory, Department of Human Genetics, KU Leuven, 3000 Leuven, Belgium and [17]Bundeswehr Institute of Radiobiology, 80937 Munich, Germany

*To whom correspondence should be addressed at: School of Medicine and The Robinson Research Institute, The University of Adelaide, Adelaide, SA 5000, Australia. Tel: +61 883133245; Fax: +61 881617342; Email: jozef.gecz@adelaide.edu.au

Received: August 10, 2015. **Revised:** September 17, 2015. **Accepted:** September 28, 2015

Abstract

Next generation genomic technologies have made a significant contribution to the understanding of the genetic architecture of human neurodevelopmental disorders. Copy number variants (CNVs) play an important role in the genetics of intellectual disability (ID). For many CNVs, and copy number gains in particular, the responsible dosage-sensitive gene(s) have been hard to identify. We have collected 18 different interstitial microduplications and 1 microtriplication of Xq25. There were 15 affected individuals from 6 different families and 13 singleton cases, 28 affected males in total. The critical overlapping region involved the *STAG2* gene, which codes for a subunit of the cohesin complex that regulates cohesion of sister chromatids and gene transcription. We demonstrate that *STAG2* is the dosage-sensitive gene within these CNVs, as gains of *STAG2* mRNA and protein dysregulate disease-relevant neuronal gene networks in cells derived from affected individuals. We also show that *STAG2* gains result in increased expression of *OPHN1*, a known X-chromosome ID gene. Overall, we define a novel cohesinopathy due to copy number gain of Xq25 and *STAG2* in particular.

Introduction

Intellectual disability (ID) is a heterogeneous neurodevelopmental disorder (NDD) of major societal and personal importance. It is at least 50% genetic, and the underlying etiology is complex and highly heterogeneous with thousands of genes and loci likely involved. It is estimated that copy number variants (CNVs) are responsible for ~21–25% of individuals with ID (1,2). Determining the clinical significance of CNVs is challenging, in particular those involving the X chromosome (3). Chromosome X duplications may lead to disease in males due to functional disomy of the duplicated genes (4). Depending on the pattern of X chromosome inactivation, heterozygous females can also be variably affected (5). Array comparative genomic hybridization (aCGH) detects X-chromosome CNVs in 0–5% of unselected individuals with NDDs (3). Of these, duplications of Xq28 including *MECP2* are the most frequent (6). In addition, duplications of Xq25 encompassing part (7–9) or all (10) of *GRIA3*, an established XLID gene (11,12), have been associated with clinically variable ID phenotype. More recently, Xq25 duplications involving *THOC2*, *XIAP*, *STAG2* or *SH2D1A*, which are located distal to *GRIA3*, have been implicated in ID (10,13–15). However, the dosage-sensitive gene or genes driving the disease phenotype in affected individuals have remained elusive. Here, we present data from systematic and in-depth clinical and molecular studies of 28 affected males (15 from 6 unrelated families and 13 singleton cases) harboring Xq25 microduplications and one case of a triplication showing that *STAG2* is the dosage-sensitive gene in the affected individuals. Our results define a novel cohesinopathy due to copy number gain of Xq25 and *STAG2* in particular.

Results

STAG2 copy number gains are implicated in intellectual disability and behavioral problems

Initially, we identified Xq25 microduplications and one microtriplication in six unrelated index males with ID and various additional clinical features through aCGH (families NSW, SA1 and SA2) and X-chromosome exome sequencing as previously described (16–18) (families D57, D166 and L70). The duplicated regions varied from 202 to 746 kb in length and contained *THOC2-XIAP-STAG2*, *XIAP-STAG2* or partial *XIAP* and *STAG2*. The triplicated region contained *XIAP* and *STAG2* (Fig. 1A). We confirmed the copy number gains by quantitative polymerase chain reaction (qPCR), high-resolution aCGH and fluorescent *in situ* hybridization (FISH), and where available, tested their segregation in extended pedigrees (Fig. 2 and *data available on request*). All procedures followed were in accordance with the ethical standards of the appropriate institutional Human Research Ethics Committees, and proper informed consent was obtained.

Subsequently, we evaluated ~27 000 males with neurodevelopmental delay and/or congenital anomalies (and 6459 male controls) referred for clinical aCGH testing and identified an additional 13 sporadic singleton cases with a duplication encompassing *STAG2*. In addition to *STAG2*, *GRIA3* was duplicated in one, *THOC2* in two, *XIAP* in six and *SH2D1A* in one individual (Fig. 1B; Signature Genomics and Baylor College of Medicine). In addition, three individuals with only *STAG2* and one individual with *STAG2-SH2D1A* and partial *TENM1* duplication were identified in the DECIPHER database (Fig. 1B). Taken together, we show that in all affected individuals, the critical region contains *STAG2*. This led us to hypothesize that *STAG2* gains might play a role in abnormal development and that *STAG2* is the disease-relevant gene in Xq25 duplications (7–10,13,14), and not *GRIA3* as previously speculated (7,10). To test our hypothesis of the importance of *STAG2* dosage for normal neuronal development, we clinically evaluated all affected individuals from the initial six families and compared them with previously published cases. We also performed *STAG2* expression analysis at the mRNA and protein level using cells derived from affected individuals.

The clinical details of our and published cases with Xq25 microduplications and their family members (total 43; males 33) are presented in Table 1 and Supplementary Material, Table S1. Clinical description of the SA1 family with Xq25 triplication is highlighted in Supplementary Material, Table S1. Photographs of the affected individuals are shown in Figure 2. We have also reviewed the clinical findings of 18 males from the literature together with the DECIPHER cases 250 183 and 270 242 (7,10,13–15,19), who all carry an Xq25 duplication encompassing *STAG2*. All males with Xq25 duplications presented with some degree of ID, mostly mild–moderate ID. Of the carrier females ($n = 10$), one had mild ID, six were described as having borderline ID or delays and the remaining three had normal cognitive function. Behavioral problems such as anxiety, hyperactivity and aggressive behavior were noted in 68% (19/28) of all affected males. Autism spectrum disorder was reported in four males. Short stature was noted in 21% (6/28) of cases for whom information was available. Head circumference was typically in the normal range. Seizures were only noted in 32% (10/31) males, excepting one female. Brain imaging was performed in 10 individuals; 4 were reported as normal and among the 6 with abnormalities, cerebellar vermis hypoplasia were noted in 4, a thin corpus callosum in 3 and prominent subarachnoid spaces in 2. Facial features were not clearly documented in all cases; however, there is evidence of a subtle, but consistent phenotype including malar flatness, full lips and prognathia was present in 23/27, 15/26 and 16/26, respectively. Recently, clinical information and photographs of six affected children carrying *STAG2* duplications has been reported (19), and many of the features overlap with adult faces

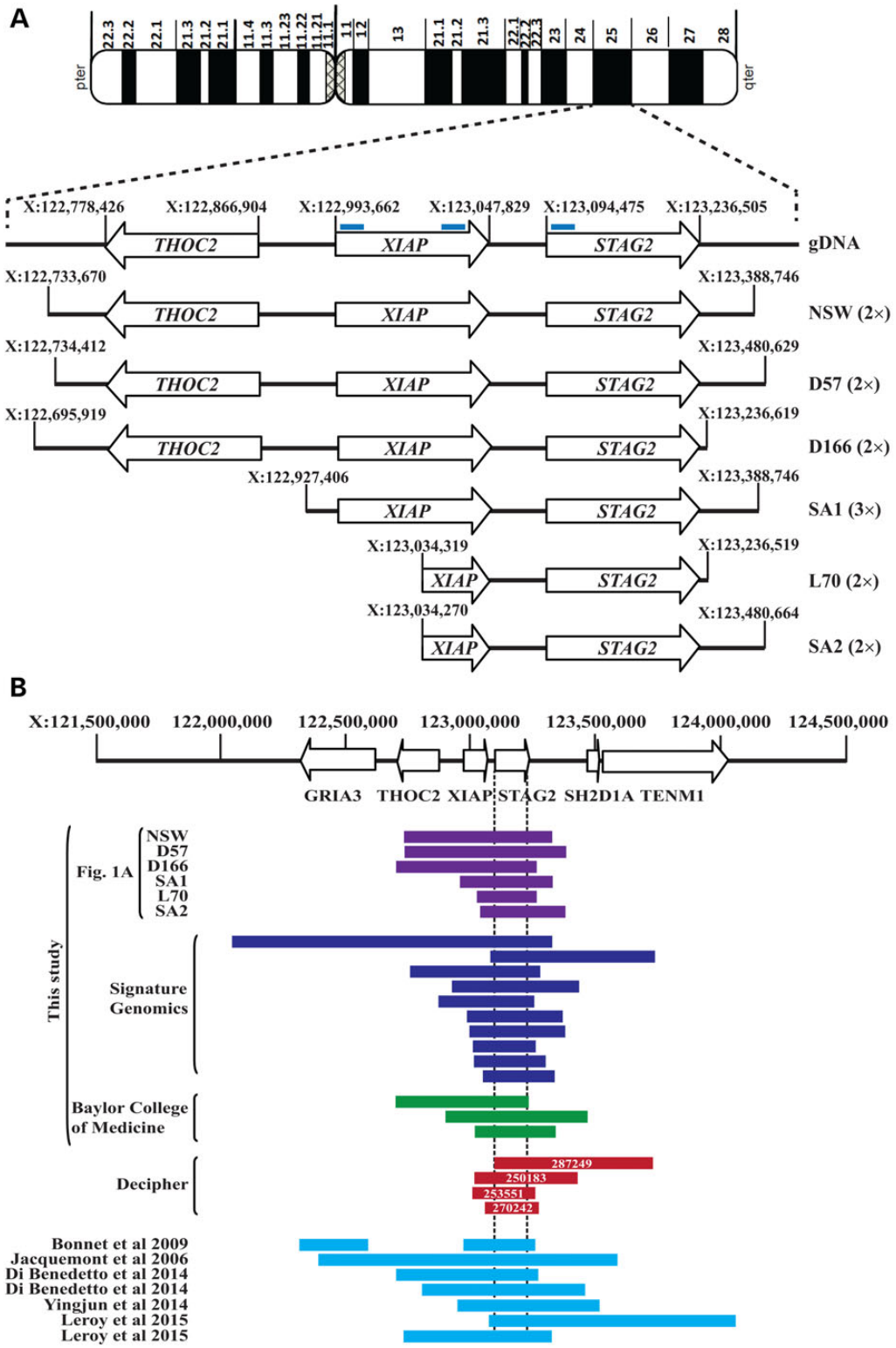

Figure 1. Summary of Xq25 copy number gains. (**A**) Detailed description of five microduplications and a microtriplication of Xq25. Duplications and triplications were identified by aCGH array (NSW, SA1 and SA2) or X-chromosome exome sequencing (D57, D166 and L70). Gene dosage was experimentally validated using the Taqman assays (probe locations shown as blue lines above the *XIAP* and *STAG2* genes). *STAG2* is common to all copy number gains. gDNA, genomic DNA. 2×, duplication; 3×, triplication. (**B**) Overview of our and published Xq25 copy number gains. Note that the shortest region of overlap includes *STAG2*. Positions are according to UCSC hg19. Xq25 carrying a partial *GRIA3* duplication in an individual with autism spectrum disorder (9) and an ID-associated 5.02 Mb duplication carrying a number of genes (10) are not shown.

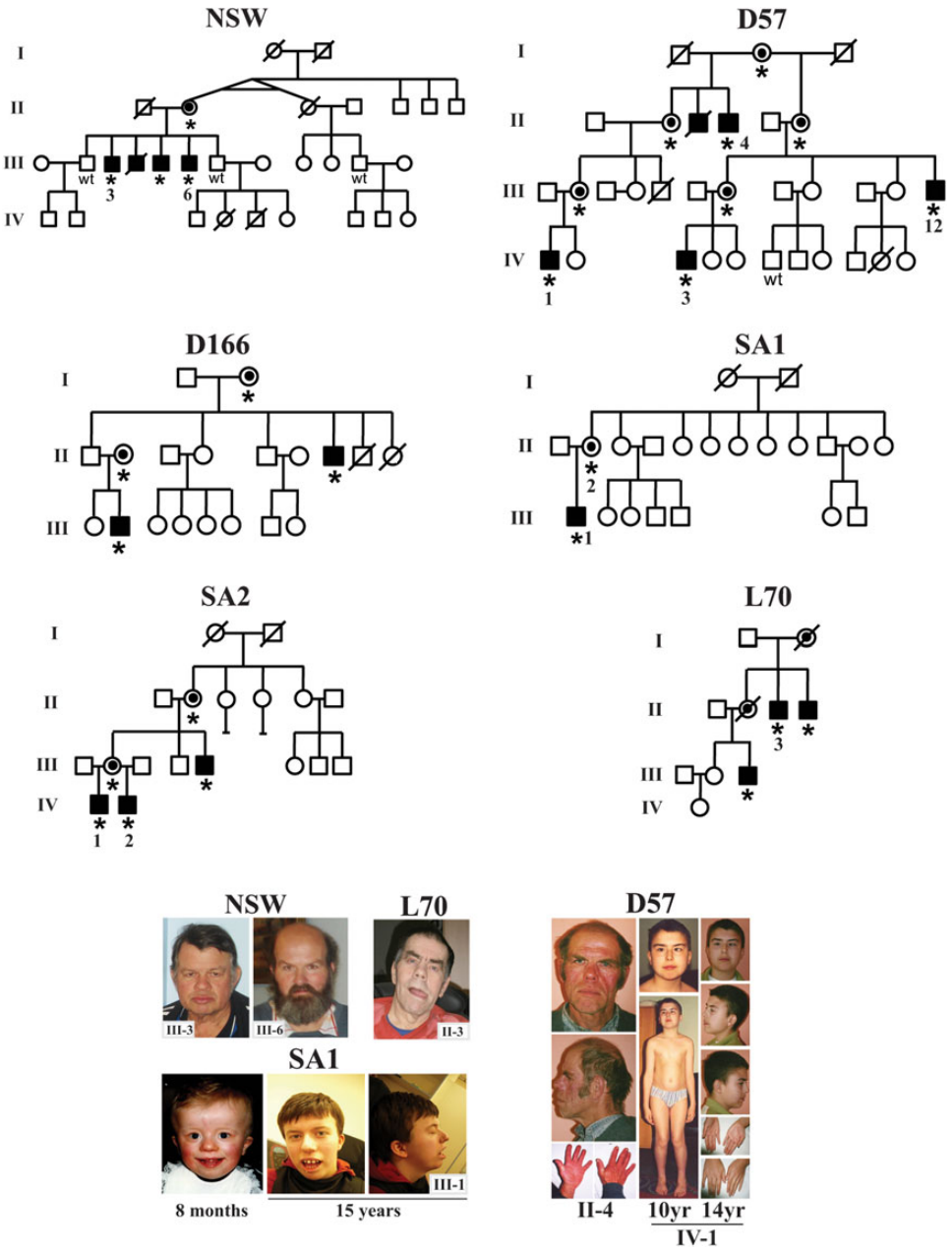

Figure 2. Pedigrees of families with Xq25 copy number gains. Pedigrees of six ID families with microduplications or a microtriplication at Xq25 including ***THOC2***, ***XIAP*** and/or ***STAG2***. *Microduplication/microtriplication carrier; wt, does not carry microduplication/microtriplication. Front and side facial views of the affected individuals are shown (photographs published with consent).

shown here, although the thin arched eyebrows and facial hypotonia are less apparent with age.

The affected male of family SA1 who carries a triplication of *XIAP* and *STAG2* had a more severe clinical phenotype compared with individuals with Xq25 duplication. He presented with severe ID, stereotypies, obsessive-compulsive behavior, anxiety and aggressive outbursts. He was dysmorphic, with a broad forehead, frontal bossing, small posteriorly rotated low-set ears, long nose, smooth philtrum, wide spaced teeth, gum hypertrophy, facial hypotonia, short distal phalanges of fingers and 2–3 toes syndactyly. He also had hypermetropia, tight Achilles tendons and valgus foot deformity. Imaging demonstrated cone-shaped epiphyses of toes 2–4 and mild cerebral ventricular enlargement with prominent subarachnoid spaces. The mother, who has four copies of the region, had slightly skewed X-inactivation (85:15) and had borderline ID and schizophrenia.

STAG2 and XIAP but not THOC2 protein levels reflect their copy number gains in patient-derived cells

To identify the dosage-sensitive gene(s), we assayed *STAG2*, *XIAP* and *THOC2* mRNA and protein expression in lymphoblastoid cell lines (immortalized B-lymphocytes, LCLs) derived from one affected individual of each of the NSW, SA1, D57 and L70 families and five male controls. Compared with controls, *STAG2* mRNA expression was increased in all four LCLs derived from the affected individuals, while *XIAP* expression was higher in LCLs from the NSW, SA1 and D57 families, and *THOC2* expression was elevated

Table 1. Summary of typical clinical features in affected males

Typical clinical features	Affected/accessible data (%)
Duplications and a triplication	$n = 33$
ID	
Borderline or not specified type	3/33 (9)
Mild/mild–moderate	16/33 (48)
Moderate	12/33 (36)
Severe	2/33 (6)
Autism spectrum disorder	4/15 (27)
Seizures	10/31 (32)
Behavior problems	19/28 (68)
Malar flatness	23/27 (85)
Thick vermillion	15/26 (58)
Facial hypotonia	16/27 (59)
Prognathism	16/26 (62)
Heavy eyebrows	7/17 (41)
Head circumference (OFC)	
Normal	22/27 (81)
OFC < P10	1/27 (4)
OFC > P90	4/27 (15)
Height	
Normal	19/28 (68)
Short stature	6/28 (21)
Tall stature	3/28 (11)

in LCLs from the NSW and D57 families (Supplementary Material, Fig. S1). These results showed that the expression of all duplicated and triplicated genes is significantly increased reflecting the copy number gains and that partial duplication of *XIAP* present in family L70 did not disrupt *XIAP* gene expression (Supplementary Material, Fig. S1). Subsequent western blot analysis of cell lysates revealed increased amounts of STAG2 and XIAP protein in affected males from the NSW, SA1 and D57 families and only an elevated STAG2 level in the affected male from family L70 (Fig. 3). In contrast, THOC2 protein levels remained unchanged in all LCLs, including the NSW and D57 families, which carry *THOC2* duplications (Fig. 3). This suggests that normal THOC2 protein levels in these LCLs are maintained by other means. We have evidence that post-translational regulation, potentially through proteasome-mediated degradation given THOC2 has been shown to be ubiquitylated (20), might be involved (21). Taken together, these results suggest that *THOC2* is not implicated in the phenotype associated with Xq25 copy number gains. *XIAP* involvement cannot be fully excluded, but it is less likely given the individual from family L70 who has normal XIAP protein levels (see Fig. 3B). Therefore, we hypothesized that copy number gains of *STAG2* alone could be responsible for the phenotype.

Transcriptome is dysregulated in patient-derived cells

To test our hypothesis, we performed transcriptome analysis on LCL-derived mRNA of one affected male from the NSW, D57, SA1 and L70 families and five male controls. We and others have demonstrated that RNA-seq analysis on patient-derived cells can provide meaningful results for the understanding of normal brain function and development (22,23). RNA-seq analyses showed that in comparison with control LCLs, 214 genes were significantly dysregulated (126 up- and 88 down-regulated; false discovery rate (FDR) < 0.1) in the four LCLs with Xq25 duplication or triplication (Supplementary Material, Table S2). We validated our RNA-seq analyses by testing a set of dysregulated genes using real-time reverse transcriptase (RT)-qPCR (Figs. 4 and 5A).

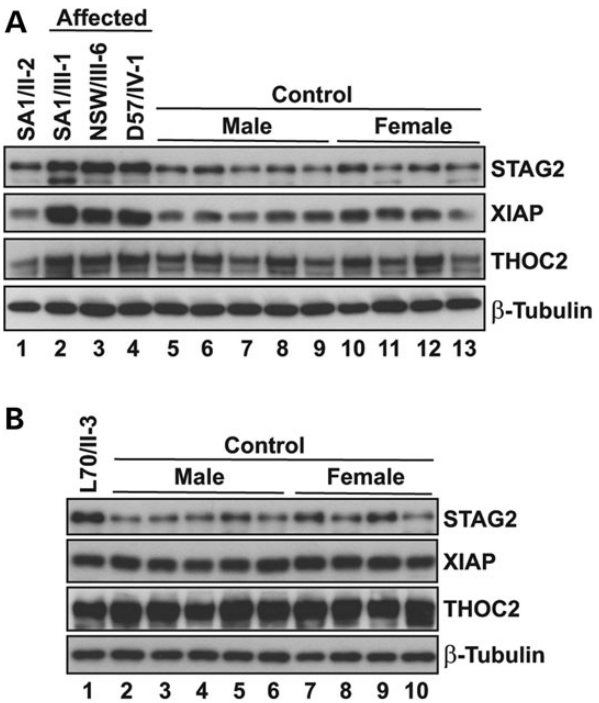

Figure 3. Endogenous XIAP and STAG2 but not THOC2 protein levels are increased in Xq25 copy number gains. Western blot analysis of THOC2, XIAP and STAG2 proteins using affected individual (**A**: SA1, NSW and D57 and **B**: L70) and control LCLs. While levels of THOC2 were unaltered in the affected LCLs with *THOC2* duplication (NSW, D57), increased XIAP and STAG2 levels reflected their genomic copy number gains (SA1, NSW, D57, L70). SA1 mother (with four copies of *XIAP-STAG2*; Lane 1, Panel A) of affected male (with three copies of *XIAP-STAG2*; Lane 2, Panel A) had XIAP and STAG2 protein comparable with the control LCLs.

These included *SLCO4C1* ($\log_2$ fold change −1.5, $P < 0.01$), encoding solute carrier organic anion transporter (OATP) family member 4C1, a member of the OATP family, which is involved in membrane transport of bile acids, conjugated steroids, thyroid hormone, eicosanoids, peptides and numerous drugs in many tissues (25); *CMTM7* ($\log_2$ fold change 3.4, $P < 4.5 \times 10^{-6}$), encoding CKLF-like marvel transmembrane domain-containing 7 the exact function of which is unknown (26); and *OPHN1* ($\log_2$ fold change 4.1, $P < 3 \times 10^{-5}$), encoding a Rho-GTPase-activating protein, important for dendritic morphogenesis and synaptic function (Fig. 5A). Compared with the controls, LCLs with duplications showed significantly higher *OPHN1* expression, which was even higher in SA1 LCLs with a *XIAP-STAG2* triplication (Fig. 5A). *OPHN1* is a known disease gene, whose loss-of-function mutations are responsible for XLID with cerebellar hypoplasia and distinctive facial dysmorphisms. To investigate whether increased *OPHN1* expression results from higher cellular levels of STAG2, XIAP or both, we measured the levels of *OPHN1* mRNA in HEK293T cells overexpressing epitope-tagged STAG2, XIAP or vector only. Significant increase in *OPHN1* mRNA was observed in STAG2, but not XIAP overexpressing HEK293T cells (Fig. 5B). These results suggest that the clinical phenotype associated with Xq25 gains could at least partly be due to *OPHN1* overexpression.

Copy number gains dysregulate disease-relevant neuronal gene networks in patient-derived cells

To determine the biological and functional relevance of the significantly dysregulated genes in LCLs from the affected

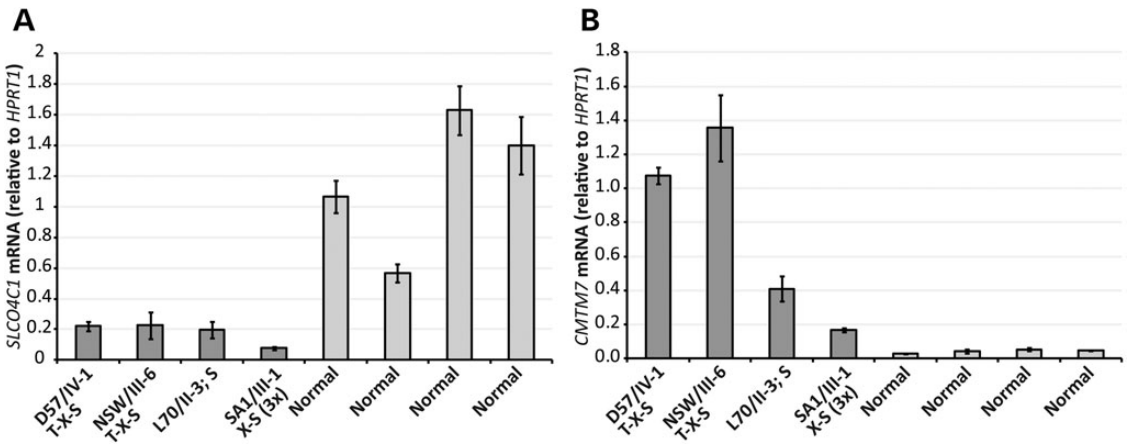

Figure 4. Xq25 copy number gains and gene dysregulation. The differentially expressed genes were identified by RNA-Seq analysis of total RNA extracted from LCLs derived from one affected individual of NSW, D57, SA1 and L70 and five control LCLs (see the Materials and Methods section). Total RNA reverse transcribed with SuperScript III reverse transcriptase was used for validating the *SCLO4C1* (**A**) and *CMTM7* (**B**). *SCLO4C1* and *CMTM7* expression was assayed by RT-qPCR using SYBR Green master mix and primer pairs listed in Supplementary Material, Table S4 and normalized to expression of *HPRT1* housekeeping gene. T-X-S, *THOC2-XIAP-STAG2*.

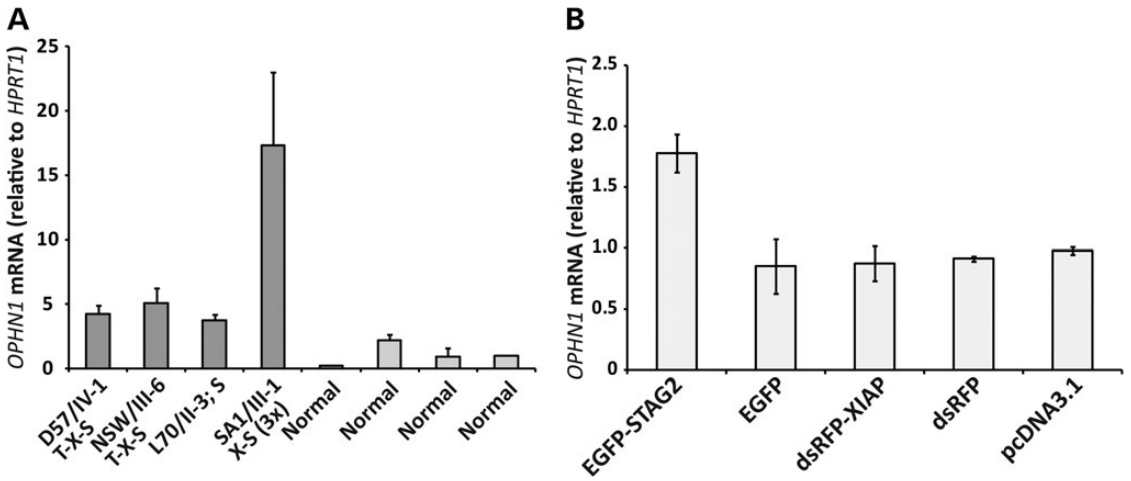

Figure 5. *OPHN1* mRNA levels are significantly increased in cells expressing high levels of STAG2 protein. (**A**) RT-qPCR assay showing significantly higher *OPHN1* expression in LCLs from the affected males with *STAG2* copy number gains ($P < 0.002$). *OPHN1* expression was assayed by RT-qPCR using the Taqman approach (Supplementary Material, Table S4) and normalized to the housekeeping *RNaseP* gene expression. T-X-S, *THOC2-XIAP-STAG2*. (**B**) *OPHN1* expression is induced in HEK293T cells overexpressing recombinant epitope-tagged STAG2 (EGFP-STAG2 versus pEGFP-C1, $P < 0.03$) but not in cells overexpressing the XIAP protein. Cells were transfected with the plasmids as shown and harvested 24 h later. One half of the cells were western blotted (24) with mouse anti-EGFP (Roche) or rabbit anti-RFP (Life Technologies) and appropriate HRP-conjugated secondary antibodies to confirm EGFP-STAG2, EGFP, dsRFP-XIAP and dsRFP expression (Supplementary Material, Fig. S3). Probing for β-tubulin was used to confirm even loading of protein samples. The other half was used for extracting total RNA that was used for RT-qPCR assay to determine *OPHN1* mRNA levels using a Taqman approach.

males with Xq25 copy number gains, we performed computational ingenuity pathway analysis using the 214 significantly (FDR < 0.1) differentially expressed genes (Supplementary Material, Table S2). This analysis identified networks of genes with functions in development of neurons ($P < 0.0008$), neuron viability ($P < 0.002$), seizures ($P < 0.0002$), disorder of basal ganglia ($P < 0.001$), neuronal cell death ($P < 0.0003$), formation of forebrain ($P < 0.001$) and movement disorders ($P < 0.0001$); neurological disease, cell-to-cell signaling, and interaction and inflammatory response (Network 3) and neurological disease, organismal injury and abnormalities (Network 4) (Supplementary Material, Fig. S2). In an independent analysis using WEB-based GEne SeT AnaLysis Toolkit (27), the differentially expressed genes were grouped into categories such as global developmental delay (17 genes), cognitive impairment (33 genes) and encephalopathy (4 genes). Finally, we observed several other genes with known involvement in neuronal processes among the differentially expressed genes. Mutations in many of these are associated with ID, developmental delay, epilepsy or neuropsychiatric disorders (e.g. ***COL4A2***, ***GPR98***, ***TSPAN7*** or ***TUBB2B*** and ***2A***, Supplementary Material, Tables S2 and S3). Taken together, these results reinforce deleterious molecular and likely also cellular consequences of increased dosage of STAG2.

Discussion

We have identified 28 affected males (15 from our 6 unrelated families and 13 others; excluding cases from the DECIPHER database) with copy number gains at Xq25 that are associated with ID, behavioral problems, seizures, malar flatness and prognathism. The copy number gains involved one or more genes: *STAG2* (28 cases), *XIAP* (17 cases), *THOC2* (12 cases) and *GRIA3* (1 case),

which are all expressed in the human brain (28). One of the rarely duplicated genes is *GRIA3*, which encodes glutamate receptor ionotropic AMPA subunit 3. Loss of function of *GRIA3* due to gene truncation by a chromosome translocation, missense variants, partial tandem duplication or a microduplication located 874 kb upstream of *GRIA3* has been linked to bipolar affective disorder and XLID (8,11,12,29,30). THOC2 protein functions as a component of the mRNA transcription/export (TREX) complex (31,32). TREX transiently binds the capped, spliced and processed mRNAs, allowing binding of additional proteins that facilitate export of mRNA from the nucleus to the cytoplasm (33). While our data show that *THOC2* loss-of-function variants cause XLID (21), the results of this study show that increased genomic dosage of *THOC2* is probably not deleterious. Firstly, *THOC2* is not duplicated in 16/28 affected males, and secondly, THOC2 protein level is not increased in the affected individuals with *THOC2* duplications. *XIAP* (X-linked inhibitor of apoptosis), also called *BIRC4*, is a member of inhibitors of apoptosis family of proteins that, besides its major role in apoptotic regulation, performs diverse biological functions, mainly through its E3 ubiquitin ligase activity (34). XIAP has a neuroprotective role; particularly in response to injury to the developing brain (35,36), its expression is reduced in Huntington's disease brain tissues (37) and loss-of-function mutations cause X-linked lymphoproliferative syndrome (38). *XIAP* expression is affected in all but one Xq25 duplication cases we tested, that of family L70, and in many other cases, *XIAP* was not even involved in the duplicated region. Based on our aggregate clinical, genetic, molecular and mRNA expression studies, we conclude that *STAG2* is the dosage-sensitive gene in Xq25 microduplications.

Detailed clinical assessment of the newly identified patients with Xq25 duplications as part of our study along with those reported earlier (Table 1 and Supplementary Material, Table S1) reinforces previously suggested phenotypic hallmarks (7,10,13–15,19). The question whether the individuals with different size Xq25 duplication and as such gene content are clinically different is highly relevant. While deriving firm conclusions will require more patients and extensive reevaluation of clinical data, patients with *STAG2* gene only duplications appear to be generally less severely affected.

STAG2 codes for a subunit of the cohesin complex that is essential for many cellular functions such as sister chromatid cohesion and segregation (canonical roles) and maintenance of chromatin architecture, DNA replication, DNA repair and transcriptional regulation (non-canonical roles) (39). Interestingly and very much in line with our results, cohesin also has multiple transcriptional roles and is tightly regulated. Minor changes in cohesin activity cause the NDD Cornelia de Lange syndrome (CdLS) that presents with phenotypic variability, including ID, facial dysmorphism, growth delay, limb abnormalities and other phenotypes (40,41). Notably, duplication involving the *SMC1A* gene, which encodes a cohesin complex subunit, is shown to be associated with growth retardation, muscular skeletal abnormalities and ID, all features seen in other cohesin disorders, CdLS is one such disorder (42). Several studies indicate that cohesin regulates transcription by facilitating insulator and enhancer–promoter looping, and by controlling the transition of promoter-proximal paused Pol II to efficient elongation (43). STAG2, or in some cases STAG1, which is mutually exclusive with STAG2, is the only cohesin subunit interacting directly with the zinc finger DNA-binding protein CTCF. This interaction bridges cohesin with CTCF, which is required for cohesin-dependent insulation activity (44) and has also been directly and indirectly implicated in ID (45,46). Recently, deleterious variants of *STAG1* have been reported in two individuals with ID, and in one of them, cognitive impairment is accompanied by behavioral problems including autism, anxiety, mood instability and aggressive outbursts (47,48). Cohesin also interacts with the mediator complex, a transcriptional coactivator and STAG1, which physically interacts with the pluripotency transcription factor Nanog (49). Furthermore, gene mutations in core and regulatory cohesin proteins have been identified in a wide range of cancers, where *STAG2* was the most frequently mutated gene (50). Whereas many cancers were caused by *STAG2*-inactivating mutations that caused chromosomal instability, some cancer types with normal karyotype could only be explained by dysregulation of gene expression, and *STAG2* mutations can be involved. Thus far no *STAG2* loss-of-function or point mutations have been identified in individuals with NDD and more specifically in cohesin-associated syndromes like CdLS (51), apart from one *de novo* missense mutation picked up by the recent DDD UK study (52). Taken together, tight regulation of cohesin core subunits and regulatory genes is essential for normal cell division and gene expression, and their dysregulation results in related NDDs termed cohesinopathies, although affected individuals have no overt defects in chromosome segregation; instead, they have altered gene expression in hundreds of genes, suggesting that the pathology of these disorders is independent of cohesin's role in sister chromatid cohesion. Given our results showing that many of the dysregulated genes of the affected individuals with *STAG2* duplications are expressed in the brain and have critical roles in the development of the nervous system (Supplementary Material, Tables S2 and S3 and Fig. S2), we can speculate that *STAG2* increased expression leads to another form of cohesinopathy.

Using RNA-Seq, we identified several differentially expressed genes in the lymphoblasts of the patients with Xq25 copy number gains. Among the most significantly dysregulated genes were those that have been implicated in various neurological disorders with ID, e.g. *TUBB2B* (OMIM #610031) and *2A* (OMIM #615763), *COL4A2* (OMIM #614483), *GPR98* (OMIM #605472), *TSPAN7* (OMIM #300210) or *OPHN1* (OMIM #300486). We followed up on one of these, *OPHN1*, which we discovered to be up-regulated in LCLs from affected individuals of the NSW, D57, L70 and SA1 families. *OPHN1* is highly expressed in the brain (53) and important for regulation of dendritic morphogenesis and synaptic plasticity (53–55). Loss-of-function mutations in *OPHN1* are responsible for syndromic XLID with cerebellar hypoplasia, variable epilepsy and distinctive facial dysmorphisms (56). In contrast, individuals who carry a duplication including *OPHN1* had a different and distinctive phenotype. A maternally inherited Xq12q13.1 duplication encompassing *OPHN1*, *YIPF6* and *STARD8* has been reported in a male with severe ID, language impairment and apparent dysmorphisms (57). A duplication encompassing *OPHN1*, *YIPF6*, *STARD8*, *EFNB1* and *PJA1* has been reported in a male with speech delay, developmental delay and facial dysmorphic features (58), and a large duplication (Xq12q13.3) including *OPHN1* has been reported in severely affected male siblings with global developmental delay and autism (59). These data are consistent with a hypothesis that higher *OPHN1* expression in individuals carrying *STAG2* copy number gains may contribute to their clinical presentations. Furthermore, *OPHN1* overexpression in rat pyramidal neurons was shown to enhance AMPA receptor-mediated transmission, and significantly increased spine size without altering the spine density (54). While perturbed STAG2-mediated OPHN1 signaling likely contributes to the cognitive impairment in individuals with Xq25 copy number gains, contributions of the other likely involved genes (see above and Supplementary Material,

Tables S2 and S3) also need to be considered and investigated in order to determine the most likely drivers of the clinical phenotype.

Broad diagnostic and research application of new genomic technologies has dramatically accelerated the discovery of microdeletions and microduplications associated with NDDs (60). There are now many examples of dosage-sensitive loci showing both deletion and duplication phenotypes, with the deletion phenotypes typically more severe than the duplication phenotypes (61–63). However, the identification of the dosage-sensitive gene (s) has been challenging. Our clinical, genetic and molecular data provide strong evidence that *STAG2* is the dosage-sensitive gene that is responsible for a novel cohesinopathy with ID, behavioral problems and other clinical presentations seen with Xq25 copy number gains.

Materials and Methods

Generation and maintenance of LCLs

The Epstein–Barr virus (EBV)-immortalized B-cell lines (LCLs) were established from peripheral blood lymphocytes of patients and controls following published method (64). Briefly, lymphocytes were isolated from 5 to 10 ml of whole blood using lymphoprep reagent following the manufacturer's protocol (GE Life Sciences, Australia) and cultured for a period of 2 weeks in RPMI 1640 (Sigma-Aldrich, NSW, Australia) supplemented with 20% fetal calf sera (FCS), 2 mM L-glutamine and 0.017 mg/ml benzylpenicillin in the presence of EBV and 0.001 mg/ml Cyclosporin A (Sigma). Once established, the LCLs were maintained in RPMI 1640 supplemented with 10% FCS, 2 mM L-glutamine and 0.017 mg/ml benzylpenicillin at the conditions 37°C with 5% CO_2.

RNA-Seq and RT-qPCR analyses

Total RNA was isolated from LCLs derived from one affected individual of NSW, D57, SA1 and L70 and five control LCLs using Quick RNeasy mini kit (Qiagen, VIC, Australia). The cDNA libraries were prepared with the Illumina TruSeq LT protocol using 2 μg RNA per sample and sequenced on the Illumina HiSeq 2000 (Illumina, San Diego, CA, USA). Approximately, 80 million pair-end reads per sample were mapped to the Hg19 build of the human genome using Tophat (version 2.0.9). HTSeq (version 0.5.4p5) was used to generate the raw counts. Differentially expressed genes (FDR < 0.1) were identified by comparing the patients and controls using edgeR package (65). RT-qPCR was used for validating the differentially regulated genes in LCLs from affected individuals using mRNA-specific primers or Taqman probes (Life Technologies, VIC, Australia) (Supplementary Material, Table S4). Total RNA reverse transcribed with SuperScript III reverse transcriptase (Life Technologies) was used for assaying the levels of *OPHN1* expression by the Taqman approach. *RNaseP* was used as a housekeeping gene to normalize *OPHN1* expression. *SCLO4C1* and *CMTM7* expression was assayed by RT-qPCR using SYBR Green master mix (Bio-Rad, NSW, Australia) using primers listed in Supplementary Material, Table S4. *HPRT1* was used as a housekeeping gene for normalizing *SCLO4C1* and *CMTM7* expression.

XIAP and STAG2 expression plasmids

pEGFP-STAG2 expression plasmid was purchased from Addgene (Number 31 972). pDsRed-monomer-C1-XIAP expression plasmid was generated by cloning human XIAP-coding sequence (PCR amplified from brain cDNA with hXIAP-*Eco*RI-F and hXIAP-*Bam*HI-R primers, Supplementary Material, Table S4) in-frame with the RFP coding sequence at *Eco*RI-*Bam*HI sites of pDsRed-monomer-C1. Sequence was confirmed by Sanger sequencing using the BigDye Terminator v3.1 chemistry (Life Technologies).

Western blotting

Total LCL lysates were prepared in 50 mM Tris–HCl pH 7.5, 250 mM NaCl, 1 mM EDTA, 50 mM NaF, 0.1 mM Na_3VO_4, 1× protease inhibitors (Roche, NSW, Australia) and 1% Triton X-100, resolved on 3–8% Tris-acetate (THOC2; Life Technologies) or 7% sodium dodecyl sulfate-polyacrylamide gel electrophoresis (66) (XIAP or STAG2) gels, transferred to nitrocellulose membranes and probed with rabbit anti-XIAP (Cell Signaling, QLD, Australia), anti-STAG2 (Cell Signaling) or anti-THOC2 (Bethyl Laboratories, Montgomery, TX, USA) primary antibodies followed by donkey anti-rabbit-IgG-HRP secondary antibodies (Dako, VIC, Australia). Blots were probed with rabbit anti-β-tubulin (Abcam, VIC, Australia) to control for even loading of protein amounts. Proteins were detected by enhanced chemiluminescence reagents (GE Life Sciences).

Supplementary Material

Supplementary Material is available at *HMG* online.

Acknowledgements

The expression constructs pEGFP-STAG2 from Prof. Todd Waldman, Georgetown University School of Medicine, Washington, USA (Addgene 31972) and pcDNA3-XIAP-Myc from Prof. Guy Salvesen, Sanford-Burnham Medical Institute, La Jolla, USA (Addgene 11833) are gratefully acknowledged. The authors also thank all the participating families.

Conflict of Interest statement. None declared.

Funding

This work was supported by Channel 7 Children's Research Foundation grants to R.K., MS McLeod Research Fellowship by the WCH Foundation to M.C., National Health and Medical Research Council of Australia (grants 628952 and 1041920) to J.G. and the EU FP7 project GENCODYS (grant number 241995) to V.M.K. and H.H.

References

1. Shoukier, M., Klein, N., Auber, B., Wickert, J., Schroder, J., Zoll, B., Burfeind, P., Bartels, I., Alsat, E.A., Lingen, M. *et al.* (2013) Array CGH in patients with developmental delay or intellectual disability: are there phenotypic clues to pathogenic copy number variants? *Clin. Genet.*, **83**, 53–65.
2. Vulto-van Silfhout, A.T., Hehir-Kwa, J.Y., van Bon, B.W., Schuurs-Hoeijmakers, J.H., Meader, S., Hellebrekers, C.J., Thoonen, I.J., de Brouwer, A.P., Brunner, H.G., Webber, C. *et al.* (2013) Clinical significance of de novo and inherited copy-number variation. *Hum. Mutat.*, **34**, 1679–1687.
3. Willemsen, M.H., de Leeuw, N., de Brouwer, A.P., Pfundt, R., Hehir-Kwa, J.Y., Yntema, H.G., Nillesen, W.M., de Vries, B.B., van Bokhoven, H. and Kleefstra, T. (2012) Interpretation of clinical relevance of X-chromosome copy number variations identified in a large cohort of individuals with cognitive disorders and/or congenital anomalies. *Eur. J. Med. Genet.*, **55**, 586–598.

4. Yamamoto, T., Shimojima, K., Shimada, S., Yokochi, K., Yoshitomi, S., Yanagihara, K., Imai, K. and Okamoto, N. (2014) Clinical impacts of genomic copy number gains at Xq28. *Hum. Genome Variation*, **1**, 14001.
5. Armstrong, L., McGowan-Jordan, J., Brierley, K. and Allanson, J.E. (2003) De novo dup(X)(q22.3q26) in a girl with evidence that functional disomy of X material is the cause of her abnormal phenotype. *Am. J. Med. Genet. A*, **116A**, 71–76.
6. Van Esch, H., Bauters, M., Ignatius, J., Jansen, M., Raynaud, M., Hollanders, K., Lugtenberg, D., Bienvenu, T., Jensen, L.R., Gecz, J. *et al.* (2005) Duplication of the MECP2 region is a frequent cause of severe mental retardation and progressive neurological symptoms in males. *Am. J. Hum. Genet.*, **77**, 442–453.
7. Bonnet, C., Leheup, B., Beri, M., Philippe, C., Gregoire, M.J. and Jonveaux, P. (2009) Aberrant GRIA3 transcripts with multiexon duplications in a family with X-linked mental retardation. *Am. J. Med. Genet. A*, **149A**, 1280–1289.
8. Chiyonobu, T., Hayashi, S., Kobayashi, K., Morimoto, M., Miyanomae, Y., Nishimura, A., Nishimoto, A., Ito, C., Imoto, I., Sugimoto, T. *et al.* (2007) Partial tandem duplication of GRIA3 in a male with mental retardation. *Am. J. Med. Genet. A*, **143A**, 1448–1455.
9. Guilmatre, A., Dubourg, C., Mosca, A.L., Legallic, S., Goldenberg, A., Drouin-Garraud, V., Layet, V., Rosier, A., Briault, S., Bonnet-Brilhault, F. *et al.* (2009) Recurrent rearrangements in synaptic and neurodevelopmental genes and shared biologic pathways in schizophrenia, autism, and mental retardation. *Arch. Gen. Psychiatry*, **66**, 947–956.
10. Philippe, A., Malan, V., Jacquemont, M.L., Boddaert, N., Bonnefont, J.P., Odent, S., Munnich, A., Colleaux, L. and Cormier-Daire, V. (2013) Xq25 duplications encompassing GRIA3 and STAG2 genes in two families convey recognizable X-linked intellectual disability with distinctive facial appearance. *Am. J. Med. Genet. A*, **161A**, 1370–1375.
11. Philips, A.K., Siren, A., Avela, K., Somer, M., Peippo, M., Ahvenainen, M., Doagu, F., Arvio, M., Kaariainen, H., Van Esch, H. *et al.* (2014) X-exome sequencing in Finnish families with intellectual disability—four novel mutations and two novel syndromic phenotypes. *Orphanet. J. Rare Dis.*, **9**, 49.
12. Wu, Y., Arai, A.C., Rumbaugh, G., Srivastava, A.K., Turner, G., Hayashi, T., Suzuki, E., Jiang, Y., Zhang, L., Rodriguez, J. *et al.* (2007) Mutations in ionotropic AMPA receptor 3 alter channel properties and are associated with moderate cognitive impairment in humans. *Proc. Natl. Acad. Sci. USA.*, **104**, 18163–18168.
13. Di Benedetto, D., Musumeci, S.A., Avola, E., Alberti, A., Buono, S., Scuderi, C., Grillo, L., Galesi, O., Spalletta, A., Giudice, M.L. *et al.* (2014) Definition of minimal duplicated region encompassing the XIAP and STAG2 genes in the Xq25 microduplication syndrome. *Am. J. Med. Genet. A*, **164A**, 1923–1930.
14. Jacquemont, M.L., Sanlaville, D., Redon, R., Raoul, O., Cormier-Daire, V., Lyonnet, S., Amiel, J., Le Merrer, M., Heron, D., de Blois, M.C. *et al.* (2006) Array-based comparative genomic hybridisation identifies high frequency of cryptic chromosomal rearrangements in patients with syndromic autism spectrum disorders. *J. Med. Genet.*, **43**, 843–849.
15. Yingjun, X., Wen, T., Yujian, L., Lingling, X., Huimin, H., Qun, F. and Junhong, C. (2015) Microduplication of chromosome Xq25 encompassing STAG2 gene in a boy with intellectual disability. *Eur. J. Med. Genet.*, **58**, 116–121.
16. Hu, H., Haas, S.A., Chelly, J., Van Esch, H., Raynaud, M., de Brouwer, A.P., Weinert, S., Froyen, G., Frints, S.G., Laumonnier, F. *et al.* (2015) X-exome sequencing of 405 unresolved families identifies seven novel intellectual disability genes. *Mol. Psychiatry*, doi: 10.1038/mp.2014.193.
17. Hu, H., Wienker, T.F., Musante, L., Kalscheuer, V.M., Kahrizi, K., Najmabadi, H. and Ropers, H.H. (2014) Integrated sequence analysis pipeline provides one-stop solution for identifying disease-causing mutations. *Hum. Mutat.*, **35**, 1427–1435.
18. Love, M.I., Mysickova, A., Sun, R., Kalscheuer, V., Vingron, M. and Haas, S.A. (2011) Modeling read counts for CNV detection in exome sequencing data. *Stat. Appl. Genet. Mol. Biol.*, **10**, doi: 10.2202/1544-6115.1732.
19. Leroy, C., Jacquemont, M.L., Doray, B., Lamblin, D., Cormier-Daire, V., Philippe, A., Nusbaum, S., Patrat, C., Steffann, J., Colleaux, L. *et al.* (2015) Xq25 duplication: the crucial role of the STAG2 gene in this novel human cohesinopathy. *Clin. Genet.*, doi: 10.1111/cge.12567.
20. Lopitz-Otsoa, F., Rodriguez-Suarez, E., Aillet, F., Casado-Vela, J., Lang, V., Matthiesen, R., Elortza, F. and Rodriguez, M.S. (2012) Integrative analysis of the ubiquitin proteome isolated using tandem ubiquitin binding entities (TUBEs). *J. Proteomics*, **75**, 2998–3014.
21. Kumar, R., Corbett, M.A., van Bon, B.W., Woenig, J.A., Weir, L., Douglas, E., Friend, K.L., Gardner, A., Shaw, M., Jolly, L.A. *et al.* (2015) THOC2 mutations implicate mRNA-export pathway in X-linked intellectual disability. *Am. J. Hum. Genet.*, **97**, 302–310.
22. Nguyen, L.S., Jolly, L., Shoubridge, C., Chan, W.K., Huang, L., Laumonnier, F., Raynaud, M., Hackett, A., Field, M., Rodriguez, J. *et al.* (2012) Transcriptome profiling of UPF3B/NMD-deficient lymphoblastoid cells from patients with various forms of intellectual disability. *Mol. Psychiatry*, **17**, 1103–1115.
23. Nishimura, Y., Martin, C.L., Vazquez-Lopez, A., Spence, S.J., Alvarez-Retuerto, A.I., Sigman, M., Steindler, C., Pellegrini, S., Schanen, N.C., Warren, S.T. *et al.* (2007) Genome-wide expression profiling of lymphoblastoid cell lines distinguishes different forms of autism and reveals shared pathways. *Hum. Mol. Genet.*, **16**, 1682–1698.
24. Kumar, R., Cheney, K.M., McKirdy, R., Neilsen, P.M., Schulz, R.B., Lee, J., Cohen, J., Booker, G.W. and Callen, D.F. (2008) CBFA2T3-ZNF652 corepressor complex regulates transcription of the E-box gene HEB. *J. Biol. Chem.*, **283**, 19026–19038.
25. Mikkaichi, T., Suzuki, T., Onogawa, T., Tanemoto, M., Mizutamari, H., Okada, M., Chaki, T., Masuda, S., Tokui, T., Eto, N. *et al.* (2004) Isolation and characterization of a digoxin transporter and its rat homologue expressed in the kidney. *Proc. Natl. Acad. Sci. USA.*, **101**, 3569–3574.
26. Miyazaki, A., Yogosawa, S., Murakami, A. and Kitamura, D. (2012) Identification of CMTM7 as a transmembrane linker of BLNK and the B-cell receptor. *PLoS One*, **7**, e31829.
27. Wang, J., Duncan, D., Shi, Z. and Zhang, B. (2013) WEB-based GEne SeT AnaLysis Toolkit (WebGestalt): update 2013. *Nucleic Acids Res.*, **41**, W77–W83.
28. Uhlen, M., Fagerberg, L., Hallstrom, B.M., Lindskog, C., Oksvold, P., Mardinoglu, A., Sivertsson, A., Kampf, C., Sjostedt, E., Asplund, A. *et al.* (2015) Proteomics. Tissue-based map of the human proteome. *Science*, **347**, 1260419.
29. Bonnet, C., Masurel-Paulet, A., Khan, A.A., Beri-Dexheimer, M., Callier, P., Mugneret, F., Philippe, C., Thauvin-Robinet, C., Faivre, L. and Jonveaux, P. (2012) Exploring the potential role of disease-causing mutation in a gene desert: duplication of noncoding elements 5′ of GRIA3 is associated with GRIA3 silencing and X-linked intellectual disability. *Hum. Mutat.*, **33**, 355–358.
30. Gecz, J., Barnett, S., Liu, J., Hollway, G., Donnelly, A., Eyre, H., Eshkevari, H.S., Baltazar, R., Grunn, A., Nagaraja, R. *et al.*

(1999) Characterization of the human glutamate receptor subunit 3 gene (GRIA3), a candidate for bipolar disorder and nonspecific X-linked mental retardation. *Genomics*, **62**, 356–368.
31. Chi, B., Wang, Q., Wu, G., Tan, M., Wang, L., Shi, M., Chang, X. and Cheng, H. (2013) Aly and THO are required for assembly of the human TREX complex and association of TREX components with the spliced mRNA. *Nucleic Acids Res.*, **41**, 1294–1306.
32. Chang, C.T., Hautbergue, G.M., Walsh, M.J., Viphakone, N., van Dijk, T.B., Philipsen, S. and Wilson, S.A. (2013) Chtop is a component of the dynamic TREX mRNA export complex. *EMBO J.*, **32**, 473–486.
33. Kohler, A. and Hurt, E. (2007) Exporting RNA from the nucleus to the cytoplasm. *Nat. Rev. Mol. Cell. Biol.*, **8**, 761–773.
34. Galban, S. and Duckett, C.S. (2010) XIAP as a ubiquitin ligase in cellular signaling. *Cell Death Differ.*, **17**, 54–60.
35. Russell, J.C., Whiting, H., Szuflita, N. and Hossain, M.A. (2008) Nuclear translocation of X-linked inhibitor of apoptosis (XIAP) determines cell fate after hypoxia ischemia in neonatal brain. *J. Neurochem.*, **106**, 1357–1370.
36. West, T., Stump, M., Lodygensky, G., Neil, J.J., Deshmukh, M. and Holtzman, D.M. (2009) Lack of X-linked inhibitor of apoptosis protein leads to increased apoptosis and tissue loss following neonatal brain injury. *ASN Neuro.*, **1**, 43–53.
37. Goffredo, D., Rigamonti, D., Zuccato, C., Tartari, M., Valenza, M. and Cattaneo, E. (2005) Prevention of cytosolic IAPs degradation: a potential pharmacological target in Huntington's disease. *Pharmacol. Res.*, **52**, 140–150.
38. Rigaud, S., Fondaneche, M.C., Lambert, N., Pasquier, B., Mateo, V., Soulas, P., Galicier, L., Le Deist, F., Rieux-Laucat, F., Revy, P. *et al.* (2006) XIAP deficiency in humans causes an X-linked lymphoproliferative syndrome. *Nature*, **444**, 110–114.
39. Mehta, G.D., Kumar, R., Srivastava, S. and Ghosh, S.K. (2013) Cohesin: functions beyond sister chromatid cohesion. *FEBS Lett.*, **587**, 2299–2312.
40. Yuan, B., Pehlivan, D., Karaca, E., Patel, N., Charng, W.L., Gambin, T., Gonzaga-Jauregui, C., Sutton, V.R., Yesil, G., Bozdogan, S.T. *et al.* (2015) Global transcriptional disturbances underlie Cornelia de Lange syndrome and related phenotypes. *J. Clin. Invest.*, **125**, 636–651.
41. Horsfield, J.A., Print, C.G. and Monnich, M. (2012) Diverse developmental disorders from the one ring: distinct molecular pathways underlie the cohesinopathies. *Front. Genet.*, **3**, 171.
42. Baquero-Montoya, C., Gil-Rodriguez, M.C., Teresa-Rodrigo, M.E., Hernandez-Marcos, M., Bueno-Lozano, G., Bueno-Martinez, I., Remeseiro, S., Fernandez-Hernandez, R., Bassecourt-Serra, M., Rodriguez de Alba, M. *et al.* (2014) Could a patient with SMC1A duplication be classified as a human cohesinopathy? *Clin. Genet.*, **85**, 446–451.
43. Schaaf, C.A., Kwak, H., Koenig, A., Misulovin, Z., Gohara, D.W., Watson, A., Zhou, Y., Lis, J.T. and Dorsett, D. (2013) Genome-wide control of RNA polymerase II activity by cohesin. *PLoS Genet.*, **9**, e1003382.
44. Xiao, T., Wallace, J. and Felsenfeld, G. (2011) Specific sites in the C terminus of CTCF interact with the SA2 subunit of the cohesin complex and are required for cohesin-dependent insulation activity. *Mol. Cell. Biol.*, **31**, 2174–2183.
45. Gregor, A., Oti, M., Kouwenhoven, E.N., Hoyer, J., Sticht, H., Ekici, A.B., Kjaergaard, S., Rauch, A., Stunnenberg, H.G., Uebe, S. *et al.* (2013) De novo mutations in the genome organizer CTCF cause intellectual disability. *Am. J. Hum. Genet.*, **93**, 124–131.
46. Lanni, S., Goracci, M., Borrelli, L., Mancano, G., Chiurazzi, P., Moscato, U., Ferre, F., Helmer-Citterich, M., Tabolacci, E. and Neri, G. (2013) Role of CTCF protein in regulating FMR1 locus transcription. *PLoS Genet.*, **9**, e1003601.
47. Gilissen, C., Hehir-Kwa, J.Y., Thung, D.T., van de Vorst, M., van Bon, B.W., Willemsen, M.H., Kwint, M., Janssen, I.M., Hoischen, A., Schenck, A. *et al.* (2014) Genome sequencing identifies major causes of severe intellectual disability. *Nature*, **511**, 344–347.
48. Rauch, A., Wieczorek, D., Graf, E., Wieland, T., Endele, S., Schwarzmayr, T., Albrecht, B., Bartholdi, D., Beygo, J., Di Donato, N. *et al.* (2012) Range of genetic mutations associated with severe non-syndromic sporadic intellectual disability: an exome sequencing study. *Lancet*, **380**, 1674–1682.
49. Nitzsche, A., Paszkowski-Rogacz, M., Matarese, F., Janssen-Megens, E.M., Hubner, N.C., Schulz, H., de Vries, I., Ding, L., Huebner, N., Mann, M. *et al.* (2011) RAD21 cooperates with pluripotency transcription factors in the maintenance of embryonic stem cell identity. *PLoS One*, **6**, e19470.
50. Solomon, D.A., Kim, J.S. and Waldman, T. (2014) Cohesin gene mutations in tumorigenesis: from discovery to clinical significance. *BMB Rep.*, **47**, 299–310.
51. Deardorff, M.A., Bando, M., Nakato, R., Watrin, E., Itoh, T., Minamino, M., Saitoh, K., Komata, M., Katou, Y., Clark, D. *et al.* (2012) HDAC8 mutations in Cornelia de Lange syndrome affect the cohesin acetylation cycle. *Nature*, **489**, 313–317.
52. Deciphering Developmental Disorders Study. (2015) Large-scale discovery of novel genetic causes of developmental disorders. *Nature*, **519**, 223–228.
53. Govek, E.E., Newey, S.E., Akerman, C.J., Cross, J.R., Van der Veken, L. and Van Aelst, L. (2004) The X-linked mental retardation protein oligophrenin-1 is required for dendritic spine morphogenesis. *Nat. Neurosci.*, **7**, 364–372.
54. Nadif Kasri, N., Nakano-Kobayashi, A., Malinow, R., Li, B. and Van Aelst, L. (2009) The Rho-linked mental retardation protein oligophrenin-1 controls synapse maturation and plasticity by stabilizing AMPA receptors. *Genes Dev.*, **23**, 1289–1302.
55. Ba, W., van der Raadt, J. and Nadif Kasri, N. (2013) Rho GTPase signaling at the synapse: implications for intellectual disability. *Exp. Cell Res.*, **319**, 2368–2374.
56. Zanni, G., Saillour, Y., Nagara, M., Billuart, P., Castelnau, L., Moraine, C., Faivre, L., Bertini, E., Durr, A., Guichet, A. *et al.* (2005) Oligophrenin 1 mutations frequently cause X-linked mental retardation with cerebellar hypoplasia. *Neurology*, **65**, 1364–1369.
57. Bedeschi, M.F., Novelli, A., Bernardini, L., Parazzini, C., Bianchi, V., Torres, B., Natacci, F., Giuffrida, M.G., Ficarazzi, P., Dallapiccola, B. *et al.* (2008) Association of syndromic mental retardation with an Xq12q13.1 duplication encompassing the oligophrenin 1 gene. *Am. J. Med. Genet. A*, **146A**, 1718–1724.
58. Petit, F., Andrieux, J., Holder-Espinasse, M., Bouquillon, S., Pennaforte, T., Storme, L. and Manouvrier-Hanu, S. (2011) Xq12q13.1 microduplication encompassing the EFNB1 gene in a boy with congenital diaphragmatic hernia. *Eur. J. Med. Genet.*, **54**, e525–e527.
59. Kaya, N., Colak, D., Albakheet, A., Al-Owain, M., Abu-Dheim, N., Al-Younes, B., Al-Zahrani, J., Mukaddes, N.M., Dervent, A., Al-Dosari, N. *et al.* (2012) A novel X-linked disorder with developmental delay and autistic features. *Ann. Neurol.*, **71**, 498–508.
60. Coe, B.P., Girirajan, S. and Eichler, E.E. (2012) A genetic model for neurodevelopmental disease. *Curr. Opin. Neurobiol.*, **22**, 829–836.
61. Deak, K.L., Horn, S.R. and Rehder, C.W. (2011) The evolving picture of microdeletion/microduplication syndromes in

the age of microarray analysis: variable expressivity and genomic complexity. *Clin. Lab. Med.*, **31**, 543–564.
62. Vissers, L.E. and Stankiewicz, P. (2012) Microdeletion and microduplication syndromes. *Methods Mol. Biol.*, **838**, 29–75.
63. Adegbola, A., Musante, L., Callewaert, B., Maciel, P., Hu, H., Isidor, B., Picker-Minh, S., Caignec, C.L., Chiaie, B.D., Vanakker, O. *et al.* (2015) Redefining the MED13L syndrome. *Eur. J. Hum. Genet.*, **23**, 1308–1317.
64. Neitzel, H. (1986) A routine method for the establishment of permanent growing lymphoblastoid cell lines. *Hum. Genet.*, **73**, 320–326.
65. Robinson, M.D., McCarthy, D.J. and Smyth, G.K. (2010) edgeR: a bioconductor package for differential expression analysis of digital gene expression data. *Bioinformatics*, **26**, 139–140.
66. Laemmli, U.K. (1970) Cleavage of structural proteins during the assembly of the head of bacteriophage T4. *Nature*, **227**, 680–685.